AD 270 470

WADD TECHNICAL REPORT 61-94

TOTAL NORMAL AND TOTAL HEMISPHERICAL EMITTANCE OF POLISHED METALS

G. L. ABBOTT
N. J. ALVARES
W. J. PARKER

U. S. NAVAL RADIOLOGICAL DEFENSE LABORATORY

NOVEMBER 1961

62-2-1

XEROX

AERONAUTICAL SYSTEMS DIVISION

NOTICES

WADD TECHNICAL REPORT 61-94

TOTAL NORMAL AND TOTAL HEMISPHERICAL EMITTANCE OF POLISHED METALS

G. L. ABBOTT
N. J. ALVARES
W. J. PARKER

U. S. NAVAL RADIOLOGICAL DEFENSE LABORATORY

NOVEMBER 1961

DIRECTORATE OF MATERIALS AND PROCESSES
CONTRACT No. MIPR 33(616)-60-24
PROJECT No. 7360

AERONAUTICAL SYSTEMS DIVISION
AIR FORCE SYSTEMS COMMAND
UNITED STATES AIR FORCE
WRIGHT-PATTERSON AIR FORCE BASE, OHIO

500 - January 1962 - 19-783

FOREWORD

This report was prepared by the U. S. Naval Radiological Defense Laboratory under MIPR 33(616)60-24. This contract was initiated under Project No. 7360, "The Chemistry and Physics of Materials", Task No. 73603, "Thermodynamics and Heat Transfer". It was administered under the direction of the Directorate of Materials and Processes, Deputy for Technology, Aeronautical Systems Division, with Mr. Robert A. Winn acting as project engineer.

This report covers work conducted from January 1, 1959 to January 1, 1960.

ABSTRACT

The objective of this research is to determine the ratio of the total hemispherical to total normal emittance for various classes of surfaces in order to find correlation factors between the total normal emittance usually measured and the total hemispherical emittance which is of importance in heat transfer problems. Measurements were made on polished platinum between 800°K and 1500°K. The total hemispherical emittance was obtained from the electrical power dissipation in an electrically heated strip suspended in a vacuum of better than 10^{-4} mm Hg and its absolute temperature measured by a thermocouple. The total normal emittance was determined with a radiation thermopile. The ratio of total hemispherical to total normal emittance was also calculated directly from the angular distribution of radiation obtained by revolving the detector about an axis through the ribbon.

The total emittance of polished platinum was given to within ±5% by the following relationships:

$$\epsilon_N = 1.03 \times 10^{-4} T(^\circ K)$$

$$\epsilon_H = 1.22 \times 10^{-4} T(^\circ K)$$

where the coefficients have units of $\deg^{-1}$ and hence

$$\frac{\epsilon_H}{\epsilon_N} = 1.18$$

In addition, data were taken on the spectral emittance at 0.65 microns and on the electrical resistivity. Observations were also made on the variation of the various measured quantities with time.

PUBLICATION REVIEW

This report has been reviewed and is approved.

FOR THE COMMANDER:

Jules I. Wittebort

J. I. WITTEBORT
Chief, Thermophysics Branch
Physics Laboratory
Directorate of Materials and Processes

TABLE OF CONTENTS

PAGE

INTRODUCTION.. 1

THEORY OF THE METHOD.. 7

EXPERIMENTAL ARRANGEMENT.. 10

CALIBRATION AND PROCEDURE... 13

RESULTS... 15

DISCUSSION.. 18

LIST OF FIGURES

FIGURE PAGE

1. Schematic diagram of experimental arrangement for measuring angular distribution........ 28

2. Detail photograph of apparatus for measurement of angular distribution........ 29

3. Over-all photograph of apparatus for measurement of angular distribution........ 29

4. Schematic diagram of experimental arrangement for measurement of time dependence of emittance........ 30

5. Detail photograph of apparatus for measurement of time dependence of emittance........ 31

6. Over-all photograph of apparatus for measurement of time dependence of emittance........ 31

7. Intensity relative to normal intensity of a platinum-black surface versus angle of emittance........ 32

8. Comparison of the thermocouple and power temperatures versus current in a platinum blackened ribbon........ 33

9. Thermopile deflection (μv) versus electrical power (watts/cm) in a platinum blackened ribbon........ 34

10. Resistivity versus absolute temperature........ 35

11. Intensity relative to normal intensity versus angle of emittance........ 36

12. Intensity relative to normal intensity versus cosine of angle of emittance........ 37

13. Ratio of total hemispherical to total normal emittance versus absolute temperature........ 38

14. Ratio of total hemispherical to total normal emittance versus total normal emittance........ 39

15. Total hemispherical and total normal emittance versus absolute temperature........ 40

LIST OF FIGURES (Continued)

FIGURE PAGE

16. Total hemispherical and total normal emittance versus absolute temperature linearly extrapolated to zero.................... 41

17. Spectral emittance at 0.65 micron versus absolute temperature.. 42

18. Total emittance versus absolute temperature illustrating the effects of surface changes with time........................ 43

19. Spectral emittance at 0.65 micron versus absolute temperature illustrating the effects of surface changes with time... 44

20. Resistivity versus absolute temperature during several temperature cycles.. 45

21. Spectral emittance at 0.65 micron and total hemispherical emittance versus time at 1283°K............................ 46

22. Photomicrographs of the platinum surface: (a) as received, (b) after 4.5 hours at ≈ 1500°K, (c) scale with 100 micron separation between marks.................................... 47

23. Comparison of the total hemispherical emittance versus temperature measurements of Davisson and Weeks and NRDL....... 48

INTRODUCTION

Radiant heat transfer is especially important at very high temperatures or at the very low pressures encountered in space. The ability of a surface to lose heat by radiation is described by the product of its total hemispherical emittance, the Stefan-Boltzmann constant, and the fourth power of its absolute temperature. There is an increasingly large volume of data presently being accumulated on the total normal emittance of a variety of surfaces. Indiscriminate substitution of these data for those of total hemispherical emittance in heat transfer problems could lead to serious errors. The equating of these two emittance values is permissible only when the angular distribution from the surface obeys Lambert's cosine law. This report describes the first part of the work undertaken by NRDL to examine the relationships between these two emittance parameters for various classes of real surfaces. Up to the present time, the work has been confined to platinum.

The reliance that can be put upon high temperature emittance data in solving heat transfer problems at the present time is not very high for several reasons. Emittance measurements are inherently very difficult because high surface temperatures are hard to measure accurately, and at low temperatures background radiation is a problem. The purity level of a given material may vary or the surface may not be entirely free of contamination. The geometry of the surface may be different as a result of different preparation techniques or because of thermal etching or recrystallization. Finally the differences may simply depend on whether the quantity being measured is total normal or total hemispherical emittance. The seriousness of the situation just described is evident when one looks at the published total emittances reported for the same material as a result of different investigations.

In accordance with the Bureau of Standards[1] we are using the following definitions to define the radiating properties of surfaces. Emittance is a property of a surface; it is the ratio of the rate of emission of radiant energy to that of a blackbody radiator at the same temperature under the same conditions. Emissivity is a fundamental property of a material and is numerically equal to emittance of a specimen of the material that has an optically smooth surface and is sufficiently thick to be opaque. It is further assumed that the surface is free from contamination and the crystalline structure and its defects adjacent to the surface is the same as that of the interior. The emittance and the emissivity can be either normal or hemispherical depending upon whether the comparison with the black surface is of the intensity normal to the surface or all of the power radiated regardless of angle. They can also be either spectral or total depending upon whether the comparison is of the radiation in a narrow

---

Manuscript released by authors April 1961 for publication as a WADD Technical Report.

spectral band or whether it includes all wavelengths. The term spectral emittance, used in this report implies normal spectral emittance.

An expression for the total normal emissivity of metals at moderately low temperatures has been derived by Aschkinass[2] and Foote[3]. The theoretical formula derived by Foote and corrected according to the latest value of the second radiation constant, ($c_2 = 1.438$), appearing in the Smithsonian Tables[4] is

$$\epsilon_n = 0.578(\rho T)^{1/2} - 0.179(\rho T) + 0.44(\rho T)^{3/2} + \ldots \tag{1}$$

where T is the absolute temperature in degrees Kelvin and ρ is the resistivity in ohm cm. Taking the angular distribution into account Davisson and Weeks[5] have derived an expression for the total hemispherical emissivity of metals. With the latest value of c_2 their formula becomes

$$\epsilon_H = 0.754(\rho T)^{1/2} - 0.635(\rho T) + 0.673(\rho T)^{3/2} + \ldots \tag{2}$$

The ratio ϵ_H/ϵ_N is calculated from Equations (1) and (2) and is compared with experimental data in this report. Briefly, the principles used to derive these relationships are stated below. The total emissivity is determined from the integral

$$\epsilon = \frac{1}{\sigma T^4} \int_0^\infty \epsilon_\lambda J_\lambda d\lambda \tag{3}$$

where σ is the Stefan Boltzmann constant, ϵ_λ is the spectral emissivity, and J_λ is the Planckian spectral distribution of the radiation from a black surface. Kirchoff's law states that

$$\epsilon_{\theta,\lambda} = 1-R_{\theta,\lambda} \tag{4}$$

where $\epsilon_{\theta,\lambda}$ is the spectral emissivity in the direction θ, and $R_{\theta,\lambda}$ is the reflectivity when the angle of incidence is equal to θ. From electromagnetic theory the reflectivities, $R_{n,\theta,\lambda}$ and $R_{p,\theta,\lambda}$ for the radiation whose electric vectors are normal to and parallel to the plane of incidence respectively are given by

$$R_{n,\theta,\lambda} = \left| \frac{\cos\theta - (D-\sin^2\theta)^{1/2}}{\cos\theta + (D-\sin^2\theta)^{1/2}} \right|^2 \qquad (5)$$

$$R_{p,\theta,\lambda} = \left| \frac{(D-\sin^2\theta)^{1/2} - D\cos\theta}{(D-\sin^2\theta)^{1/2} + D\cos\theta} \right|^2 \qquad (6)$$

where D is the complex dielectric constant and

$$R_{\theta,\lambda} = \frac{R_{n,\theta,\lambda} + R_{p,\theta,\lambda}}{2} \qquad (7)$$

The imaginary component of the dielectric constant accounts for conduction and absorption within the material. Equations (3) through (7) are exact. The calculation of the complex dielectric constant is usually where the approximations are introduced.

Considering only the free electrons, the classical equations of the optical constants of metals are given by Mott and Jones[6] as

$$D' = n^2 - k^2 = 1 - \frac{4\pi Ne^2}{m}\left(\omega^2 + \frac{1}{\tau^2}\right)^{-1}$$

$$D'' = 2nk = \frac{4\pi Ne^2}{m}\,\frac{1}{\omega\tau}\left(\omega^2 + \frac{1}{\tau^2}\right)^{-1}$$

where $D = D' + iD''$ and $\tau = \dfrac{m}{Ne^2\rho}$ and

τ = relaxation time of the electron
n = index of refraction
k = extinction coefficient
N = number of free electrons per unit volume
e = electronic charge
m = electronic mass
ω = angular frequency of the electromagnetic radiation
c = velocity of light
$i = \sqrt{-1}$

If we let $y = 2\pi c\tau/\lambda = 2\pi mc/Ne^2\rho\lambda$ then

$$D = 1 - \left(\frac{y + i}{1 + y^2}\right)\frac{60\lambda}{\rho} \qquad (8)$$

where λ is the wavelength in centimeters, ρ is the d.c. resistivity in ohm cm, and $y = 1.1 \times 10^{-9}\, V/s\lambda\rho$. The units of the constant terms appearing in this report, although not explicitly stated, are understood to be those required to make the equations dimensionally correct. Here V is the atomic volume, and s is the effective number of free electrons per atom. The Hagen Rubins approximation used by Foote[3] in his derivation of the total normal emissivity is based on the assumption that

$$\frac{60\lambda}{\rho} \gg 1 \gg y$$

Davisson and Weeks[5] assumed only that $y \ll 1$. If the wavelengths are sufficiently long, it can be seen that these are both valid approximations. However, when the radiating temperature is high, the wavelengths are short and these approximations must be checked along with other smaller contributions such as internal photoelectric effect and the polarization of the electron cores. The internal photoelectric effect (which includes the ejection of electrons from the d shell and the elevation of conduction electrons into a higher zone) usually has a threshold in the visible or ultraviolet portion of the spectrum and thus is not a large factor in the radiation emitted by metals. There are, however, absorption bands in the infrared for transition metals and this serves to increase their high temperature emissivity. The electronic polarizability α_e has a resonant frequency in the ultraviolet, but in the infrared region it is essentially real and constant and equal to its steady field value. The electronic polarizability for a number of metals is given by Van Vleck.[7] Although its contribution is small ($4\pi\alpha_e = 1.3$ for silver) it is present throughout the radiating spectrum of the solid. Then Equation (8) becomes

$$D = 1 + 4\pi\alpha_e - \left(\frac{i + y}{1 + y^2}\right)\frac{60\lambda}{\rho} \tag{9}$$

Equations (1) and (2) should be accurate approximations of the model upon which they are based when the two following conditions are met throughout the spectral region over which most of the radiation occurs:

(a) $\dfrac{60\lambda}{\rho} \gg 1 + 4\pi\alpha_e$

(b) $y \ll 1$ or $\dfrac{s\lambda\rho}{V} \gg 1.1 \times 10^{-9}$

It is easier to interpret these restrictions in the present case if we note that over 99% of the radiation from a blackbody radiator occurs at wavelengths longer than $\lambda = 0.14/T$. Thus condition (a) becomes

$$(\rho T) \ll \frac{8.4}{1 + 4\pi\alpha_e}$$

It can be checked that this is not an undue restriction for most metals. By the same substitution, condition (b) becomes

$$\left(\frac{\rho}{T}\right) \gg 8 \times 10^{-9} \left(\frac{V}{s}\right) \tag{10}$$

The right hand member will be of the order of 10^{-7}. In the case of silver $s = 0.89$, $V = 10.2$, and ρ/T which is not very sensitive to temperature is about 5.5×10^{-9}. For platinum, $s = 0.6$, $V = 9.2$ while ρ/T is about 3.5×10^{-8}. Clearly, this is not a good approximation in either case and a correction to Equations (1) and (2) is desirable.

The purpose of the research described in this report is not primarily aimed at producing more emittance values for a greater number of materials over a more extended temperature range, but to explain if possible the rather wide variation in the published emittance values already in existence by making rather exhaustive measurements on a few materials. The results of this work when completed should be helpful in interpreting published emittance values and in setting up new emittance measuring systems.

In comparing the measured emittances with the theoretical emissivity which was discussed above, it is necessary to reconsider the relationships between the two quantities. The emittance is equal to the emissivity when certain conditions are met. One, the specimen must be opaque. This is not a difficult requirement to meet for metals. Two, the specimen must be free of surface contamination. This can be achieved reasonably well by cleaning and polishing the specimen and performing the measurements in a vacuum or in an inert atmosphere. Even here an adsorbed layer of gas is held at the surface except in the most extreme vacuums. However, it is assumed that this layer is too thin to be of consequence. Three, the crystalline structure and its defects at the surface must be characteristics of the material rather than a product of the surface treatment. This will always be violated to some extent by polishing or rolling. Four, the surface must be optically smooth; once the specimen is adequately polished, it will retain a smooth surface at low temperatures. However, at elevated temperature, recrystallization and thermal etching take place and the specimen appears rough to the eye. Examination of these surfaces under the microscope shows that the crystallites formed are of the order of 100 microns. Consequently, the effective surface area and the emittance becomes progressively higher with the passage of time at elevated temperatures. Emittance versus time measurements on platinum are included in this report.

Aside from the difference between emittance and emissivity, variations in measured emittance can be due to the purity of the specimens. Comparisons of the electrical resistivity can serve as a check on this point. Another possible source of variation in the reported emittance values is the difficulty of accurate temperature determinations.

The previous mechanical and temperature history of a bulk metal influences its optical properties, making it very difficult to achieve reproducible conditions for experimentation. Some investigators in this field are studying single crystals in an attempt to overcome this effect. However, they have found that minute imperfections in single crystals also cause variations in their results. Despite these problems, several theoretical ideas that describe these phenomena have been proposed. Unfortunately, they have not yielded mathematical expressions which are consistently in agreement with experiment.[8]

Any form of work done on a metal, alters the mechanical properties of the metal by distorting the crystalline structure. A portion of the energy from the applied work is stored in the deformed crystals in the form of stresses. If the metal is then heated to a temperature, commonly called the recrystallization temperature, the above process is reversed, the stored energy is released, the metal starts to recrystallize, and unstressed crystals are formed.[9] The temperature at which metal will generally start the recrystallization process is roughly 0.4 times the absolute melting point temperature.[10] The recrystallization rate, and the ultimate crystal dimensions are dependent on the amount of distortion of the original crystal matrix, and the magnitude of the applied temperature. However, this process does not proceed in a regular fashion, since the unstressed recrystallized crystal may undergo a secondary recrystallization due to a grain boundary migration, caused by an increase in temperature, restressing an unstrained crystal.[11] The impetus for recrystallization is not too well known. Somehow nuclei are formed from which crystals grow. Some investigators contend that the crystals grow from undistorted remains of the original structure, while others have stated that new lattice particles from the most disturbed areas are responsible.[12] Another opinion is that high energy crystal interfaces migrate into low energy interfaces by means of surface tension forces.[13] Still another theory is that there are present in all metals, at all times, unstressed subgrain blocks, which initiate recrystallization.[14] It is fortunate that more research is being directed to this problem.

Why and how recrystallization proceeds in a metal is of interest to this experiment because metals do not stay polished at high temperatures. Due to this recrystallization, the effective surface area and the total emittance vary not only with temperature but also with time. This effect has been observed previously;[15,16] however, it was not investigated. By referring to the literature of total normal, total hemispherical, or spectral emittance at 0.65 microns versus temperature for platinum[17,18], one finds that there are extreme variations in the published data. Although the sample purity and the original surface conditions definitely influence these variations, the surface recrystallization of the samples was probably also a contributing factor. This is a factor that can and should be more thoroughly investigated.

More knowledge of metal surfaces is necessary before individual emittance measurements can be compared to the degree of reliability desired.

THEORY OF THE METHOD

The differential equation of heat flow in an electrically heated ribbon of conducting metal is given by

$$I^2R = IE = A \frac{\partial}{\partial z}\left(K \frac{\partial T}{\partial z}\right) + DAC \frac{\partial T}{\partial t} + \epsilon_H P\sigma T^4 - \alpha P\sigma T_o^4$$

where I is the current; R, the resistance per unit length; E, the voltage per unit length; z, the distance along the ribbon; A, the cross sectional area; K, the thermal conductivity; T, the absolute temperature; D, the density; C, the heat capacity; ϵ_H, the total hemispherical emittance; P, the radiating area per unit length; σ, the Stefan Boltzmann constant; and α is the absorptivity of the ribbon at temperature T for radiation with a relative spectral distribution equal to that of a black body at the wall temperature T_o. The terms on the left side of this equation represent the power generated within the ribbon and are equated to the power dissipated by conduction and radiation plus the energy stored. The last term on the right is the power absorbed by the ribbon from its surroundings at temperature T_o. This equation does not include a convective term since a vacuum environment only will be considered. It is also assumed that the walls are non-reflecting. In a steady state condition at the center of a ribbon of sufficient length to establish a uniform temperature region, the energy will be lost by radiation only. Then this equation reduces to

$$I^2R = IE = P\sigma(\epsilon_H T^4 - \alpha\, T_o^4) = \epsilon_H P\sigma(T^4 - \frac{\alpha}{\epsilon_H}\, T_o^4)$$

It is often found that α/ϵ_H is set equal to one, or that the term $\alpha\, T_o^4/\epsilon_H$ is neglected altogether. The omission of the term will account for an error which is less than 1% when T/T_o is equal to 3 or greater, but if $T_o = 300°K$ an appreciable error may occur when dealing with ribbons at temperatures much less than 1000°K. When $\alpha\, T_o^4/\epsilon_H$ is taken into account, the problem arises as to what value to attach to α/ϵ_H. One method of reasonable approximation is to consider Equation (2). If the radiation from the surroundings at T_o is assumed to have a black body distribution, then the absorptance of the ribbon based on the free electron theory of metals at temperature T becomes

$$\alpha = a(\rho T_o)^{1/2} + b(\rho T_o) + c(\rho T_o)^{3/2} + \ldots$$

where ρ is the electrical resistivity while the emittance is

$$\epsilon_H = a(\rho T)^{1/2} + b(\rho T) + c(\rho T)^{3/2} + \ldots$$

from which

$$\frac{\alpha}{\epsilon_H} = \frac{a(\rho T_o)^{1/2} + b(\rho T_o) + \ldots}{a(\rho T)^{1/2} + b(\rho T) + \ldots}$$

$$\frac{\alpha}{\epsilon_H} \approx \left(\frac{T_o}{T}\right)^{1/2}$$

and

$$I^2R = IE = \epsilon_H P\sigma \left[T^4 - \left(\frac{T_o}{T}\right)^{1/2} T_o{}^4 \right] \qquad (11)$$

When the voltage per unit length and the current are known, both the resistivity and total hemispherical emittance may be found from Equation (11).

Thus

$$\rho = \frac{EA}{I} \qquad (12)$$

and

$$\epsilon_H = \frac{EI}{P\sigma\left[T^4 - \left(\frac{T_o}{T}\right)^{1/2} T_o{}^4\right]} \qquad (13)$$

The total normal emittance may be determined with a thermopile that has been calibrated for black body radiation by comparing the normal power of the specimen relative to that of a black body at the same temperature. Thus, the total normal emittance is:

$$\epsilon_N = \frac{Bx}{\frac{P\sigma}{\pi}\left[T^4 - \left(\frac{T_o}{T}\right)^{1/2} T_o^{\,4}\right]} \tag{14}$$

where B is the thermopile calibration constant and x is the thermopile output voltage.

Now the ratio of total hemispherical to total normal emittance may be arrived at by two methods. First, by the quotient of the emittances from Equations (13) and (14) and second, by measuring the angular distribution of radiation from a plane surface. The ratio by the first method is

$$\frac{\epsilon_H}{\epsilon_N} = \frac{\pi\ EI}{B\ x} \tag{15}$$

The calculation of this ratio by the latter method is based on the following derivation. The total radiant power emitted into a hemisphere per unit area is

$$H = \epsilon_H \sigma T^4 = \int_0^{\pi/2} \epsilon_N \frac{\sigma T^4}{\pi} f(\theta)\ 2\pi \sin\theta d\theta \tag{16}$$

where $\epsilon_N\ \sigma T^4/\pi$ is the power emitted per unit solid angle normal to the surface, $f(\theta)$ is the ratio of the intensity at angle θ to the normal intensity and $2\pi \sin\theta d\theta$ is the differential solid angle. When the assumption is made that the emitting surface is Lambertian, then $f(\theta) = \cos\theta$, but as can be seen from Equation (7), this is not valid in the case of polished metals. The expression for the ratio of total hemispherical to total normal emittance may then be written

$$\frac{\epsilon_H}{\epsilon_N} = 2\int_0^{\pi/2} f(\theta) \sin\theta d\theta = 2\int_0^{1} f(\theta) d(\cos\theta)$$

This may be numerically integrated in the form of the sum

$$\frac{\epsilon_H}{\epsilon_N} = 2\sum_{n=1}^{S} f(\theta_n)(\cos\theta_n - \cos\theta_{n+1}) = \frac{2}{S}\sum_{n=1}^{S} f(\theta_n) \tag{17}$$

where S is the number of equal increments along the cos θ axis between 0 and 1, and the θ_n are chosen such that the cosθ_n are separated by equal increments of 1/S, and $f(\theta_n)$ is the ratio of the intensity at θ_n to the normal intensity.

Since the interest here is only in relative intensity, no absolute calibration of the detector is necessary as in the case where the detector is used for direct determination of normal emittance.

The spectral emittance at 0.65 micron may also be readily determined if the true temperature and brightness temperature of the ribbon are known. On the basis of Wien's law the following relation is established

$$\epsilon_\lambda \exp(-c_2/\lambda T) = \exp(-c_2/\lambda T_A)$$

where T is the true temperature of the ribbon and T_A is the brightness temperature. This reduces to

$$\epsilon_\lambda = \exp\left[-2.211 \times 10^4 \left(\frac{T-T_A}{TT_A}\right)\right] \tag{18}$$

where $\lambda = 0.65\mu$ and $c_2 = 1.438$. Therefore, the total hemispherical emittance, total normal emittance, spectral emittance, and resistivity of a conducting ribbon may be found if the true temperature, apparent temperature, current, voltage per unit length and angular distribution of emitted energy are known.

EXPERIMENTAL ARRANGEMENT

The experimental arrangement is shown schematically in Fig. 1 and pictorially in Figs. 2 and 3. The sample under test is in the form of a ribbon 12 inches long, 1 centimeter wide, and 0.003 inch thick. The thickness of the specimen was determined by its weight and its length and width as measured by a traveling microscope. The ribbon is supported vertically in a chamber where a vacuum is maintained at better than 10^{-4} mm Hg. The lower support of ribbon is so arranged that it may be moved vertically to compensate for thermal expansion of the specimen while being rigidly held about a vertical axis. An adjustable current is passed through the diagonal control wire attached to the lower support arm, as seen in Fig. 1. The variation in wire length due to thermal expansion enables the ribbon to be kept straight without undue strain from the weight of the support.

The alternating current for heating the ribbon was supplied from a 10 to 1 step down transformer which had primary regulation and was adjusted by a variable transformer to provde a maximum output voltage of 10 volts. This current was supplied through the support arms and was measured with a 0 - 5 amp, 1% accuracy ammeter working in conjunction with a current transformer.

Two chromel-alumel, 0.005 inch thermocouples were welded to the ribbon with a separation of at least 4 cm which was of sufficient length so that the voltage per unit length (E) could be measured with reasonable precision. Either the chromel or alumel wires of each thermocouple could be switched to the input of a high impedance a.c. 10 meg VTVM for voltage measurements, or the thermocouples themselves switched to a Leeds and Northrup K-2 potentiometer for temperature determination. The two wires of each thermocouple were welded separately to the ribbon with the electrical circuit completed through the ribbon itself. The weld arrangement can be seen pictorially in Fig. 1. The weld beads were separated by about 1 mm and were placed on a line perpendicular to the current flow in order to minimize a.c. pickup in the thermocouple wires. The vertical distances of each thermocouple from the center of the ribbon were not equal so that deviations from the necessary condition of uniform temperature between them could be detected.

The detector was taken from a Minneapolis-Honeywell "Radiomatic" pyrometer and consisted of a 10 element iron constantan thermopile with a circular configuration 3 mm in diameter. It was mounted between two copper rings and enclosed in an aluminum housing, as shown in Fig. 1. The copper rings were in thermal contact, but electrically insulated by thin mica washers, from the cold junctions of the thermopile. The radiation from the ribbon entered the housing through an opening, the size of which could be adjusted for different fields of view, and impinged on the thermopile element which was coated with an aqueous solution of lamp black. An electrically operated shutter opened or closed the entrance. The inside of the housing was blackened everywhere with carbon black deposited from burning camphor to minimize reflections. The field of view was adjusted so that it was wider than the ribbon but was about 2 cm along its length (the z axis). The portion of the ribbon viewed was between the thermocouples. The voltage output of the thermopile was amplified by a d.c. microvoltmeter and measured with a digital voltmeter with an overall accuracy of less than ±1%; the system having been calibrated with a Leeds and Northrup K-2 potentiometer.

The thermopile, its housing, and shutter mechanism comprised a unit which was mounted on a post capable of being rotated through an angle of approximately 110° on either side of the normal to the ribbon; the axis of rotation being the longitudinal axis of the ribbon 13 cm from the detector. A three turn potentiometer was geared to the rotating mount to serve as an angular indicating device. A d.c. voltage was applied across the potentiometer with the electrical zero at the center of the span corresponding to the detector position normal to the ribbon. The zero position as well as the span voltage was adjustable in order to account for slight twisting of the ribbon at different temperatures. The voltage at the potentiometer sliding arm varied from -0.900 volt , through zero, to +0.900 volt as the angle was changed from 90° on one side of the normal to 90° on the other side, and was measured on a digital voltmeter with an over-all accuracy of approximately ±0.4 degree .

In the initial design of the experimental arrangement, certain precautions were taken to reduce the effect of spurious reflections on the angular distribution of radiation incident on the thermopile. Reflections from the aluminum vacuum chamber were expected, consequently, the surface was roughened by sandblasting and then black anodized. The chamber was positioned with the ribbon displaced from the center of the chamber so that the conjugate focus of the ribbon was not at the ribbon itself or the thermopile. Next, the thermopile housing and its support were constructed so that no surfaces presented themselves normal to the ribbon, and in addition a conical aluminum shield was placed in front of the thermopile housing to reduce the ambient temperature rise of the housing. The various support components within the chamber were constructed of black anodized aluminum. The nature of this experiment presented a situation, unique in that the thermopile was required to see no reflected radiation throughout a circular arc of 180°. However, it was found that at various arbitrary angles, reflections were still resulting in measurement uncertainties, particularly at the normal to the ribbon. The eventual virtual elimination of reflections came about after the following steps were taken. The reflectivity of anodized aluminum is quite high, particularly at the longer wavelengths, hence all surfaces including the chamber itself were painted with "blackboard-slating" lacquer which, due to the high emissivity of organic materials in the infrared, substantially reduced reflections at angles other than the normal. Finally, the conical surfaces of the thermopile and its heat shield were diffuse enough to cause reflections back to the ribbon and subsequent reflection to the thermopile when it was located at the normal to the ribbon. These reflections were eliminated by attaching front surfaced aluminized glass mirrors to the conical surfaces of the heat shield. This in effect reflected the radiation to other surfaces at the top and bottom of the chamber which were highly absorbing.

A second separate system similar to the one just described was used to produce additional data on emittance and particularly to observe the time dependence at various temperatures. The experimental arrangement was similar to the one just discussed except that the thermopile was stationary and only received normal radiation from the ribbon. A schematic diagram of the equipment employed in this phase of the research is shown in Fig. 4 and photographs are shown in Figs. 5 and 6. The brightness temperature of the sample was measured by a micro optical pyrometer at 0.65 micron .

All platinum sample strips used in the research were purchased from the same source, the quoted composition was commercial grade, 99.95% pure, with trace amounts of palladium, rhodium, gold, and silver present from the smelting process. The samples were cold rolled to their 3 mil thickness with a tolerance of ±5% on all dimensions. The only observable difference in the two separate orders of strips, purchased for this research was in the surface polish of the "as received" samples. The second batch was not as specular as the first. Therefore, the initial emittance was higher.

CALIBRATION AND PROCEDURE

The thermopiles in both systems were calibrated in their normal mode of operation by sensing the power radiated normally by a platinum strip blackened with electrolytically deposited platinum from a chloroplatinic acid solution. The total power radiated per unit area of surface was determined by the voltage gradient and the current through the ribbon. The principal function of the black coating was to produce a diffuse radiating surface whose radiant intensity was proportional to the cosine of the angle of emission with respect to the normal. Under these conditions the power radiated per unit solid angle normal to the surface is simply equal to the electrical power dissipated divided by π. The angular distribution of the radiation was measured by revolving the thermopile around the ribbon in the first system, whence the cosine law was followed very closely (Fig. 7). This demonstrated the reliability of the angular measurement system and the freedom from wall reflections, as well as verifying the assumption of a radiating surface which obeyed Lambert's cosine law. At 973°K and 1046°K the true temperature as determined with a thermocouple was within 1.0% of the brightness temperature measured by the disappearing filament optical pyrometer. Also the power temperature obtained by equating the electrical power dissipation and the Stefan Boltzmann radiation law was within 1% of that indicated by the thermocouple over the range of temperature from 700°K to 1100°K as shown in Fig. 8. This was a verification of the blackness of platinum black in this temperature interval. Below 700°K deviations are probably due to the semi-transparence of the black at long wavelengths. The linearity of the thermopile was checked by plotting the electrical power dissipation versus thermopile output voltage as shown in Fig. 9 up to the maximum temperature at which the black coating was stable. This breakdown occurred just above 1100°K. The total radiant power of a blackened strip at 1100°K is approximately equal to that from a polished platinum strip at 1600°K. The linearity of the thermopile over a wide ribbon temperature interval demonstrated the satisfaction of the requirement for a receiver having a flat spectral absorptivity characteristic.

In measurements up to the present time, no effort has been made to keep the thermopile housing at constant temperature, other than the heat shield; consequently, some uncertainty has been found in reliability of absolute power measurements due to the slight temperature rise of the housing during the time span of approximately one hour necessary to make a complete angular distribution measurement. Some attempt has been made to correct for this by monitoring the temperature of the thermopile cold junctions, but it appeared that the rate of change of drift was also important. Consequently, this becomes part of the over-all experimental errors of the system. In the performance of an experimental run it has been found advantageous to measure the radiant power at large angles of incidence (i.e., low incident power) early in the run. This tends to minimize the errors due to temperature changes of the thermopile enclosure. In general, a reduction of approximately 2.5% in the output voltage of the thermopile has been observed in measurements at normal incidence between the beginning and the end of a run. Efforts to eliminate this uncertainty are currently being undertaken through temperature stabilization of both the thermopile housing and the background by water circulation. The effect of this difference will be discussed in the next section.

The disappearing filament optical pyrometer was capable of measuring the brightness temperature of a spot as small as 0.001" in linear dimensions and could detect differences in temperature in the order of 1 or 2 degrees. The pyrometer was calibrated against a secondary standard blackbody furnace (emissivity of 0.99) at 1273°K and its linearity was checked by observing a tungsten ribbon filament at a higher temperature on two different pyrometer scales. The estimated accuracy of brightness temperature measurements is better than ±1%. The optical pyrometer has been used to give a more accurate indication of true temperature by observing the difference in temperature between the point of thermocouple contact and its surroundings. Assuming that the spectral emittance of the ribbon is constant over very small temperature changes, this difference may be added to that measured by the thermocouple and has amounted to about 5°C to 10°C depending on the sample involved and the temperature.

With the stationary thermopile system it was possible to measure the total hemispherical, total normal, and spectral emittance at 0.65 micron as a function of temperature. With this capability it was the initial purpose to independently compute these data and compare the results with those generated by the other phase of the project. When it became apparent that both systems were functioning properly, the emphasis of this phase was directed toward determining the variation of emittance with time. It had been observed that there was a definite change in the surface structure at high temperature due to a recrystallization. The change in emittance with time was demonstrated by differences between succeeding emittance versus temperature curves as the ribbon temperature was cycled several times between 700°K and 1500°K. Emittance measurements were also made as a function of time while the ribbon was maintained at a fixed temperature for several hours.

The total hemispherical emittance was determined from Equation (13), and the total normal emittance from Equation (14).

The spectral emittance at 0.65 micron was determined from accurate measurements of the true temperature and brightness temperature and is computed from Equation (18).

The true temperature was determined from the voltage output of the two thermocouples, and the brightness temperature was read directly from the micro-optical pyrometer.

The total normal and total hemispherical emittance was measured in three independent temperature cycles on one sample of platinum. The results of the comparison indicated a definite measurable increase in emittance with time as shown in Fig. 18. It was desirable to follow these changes more closely. Therefore, by using the same experimental set up, and holding the sample's temperature constant, it should have been possible to observe an increase of the sample's emittance with time. This experiment was performed with the two different strips at temperatures above 1000°C. The first attempt was made with the sample that had been used for the cyclic experiment and an increase in emittance was recorded. A sample strip from the second purchase order was then measured. The "as received" surface of this sample did not have the degree of polish that the previous sample from the first order had. Thus its initial emittance was noticeably higher than the first sample. This sample was run at two temperatures, and the trend of the emittance characteristics was as expected.

RESULTS

The values of emittance reported here are for a platinum strip in the "as received" condition. However, the fresh surface is quite specular to the eye and is considered in this report to be equivalent to a "polished" ribbon. We originally thought that the published values of the electrical resistivity of platinum might be used as a means for determining the temperature of the ribbon so as to avoid the possibility of the deleterious effects of a thermocouple junction on the surface. However, this proved impractical because of the wide spread in the published resistivity data as can be seen in Fig. 10. Apparently, this is due to small differences in the impurity content, as shown in the Metals Handbook.[19] After developing proper welding techniques, the only effect of the thermocouple was a slight reduction in temperature at the junction due to heat conduction along the wires. This was easily corrected for with the optical pyrometer as explained previously. The NRDL values of resistivity, determined with Equation (12) are also shown in Fig. 10 along with values from the American Institute of Physics Handbook[20] and the Smithsonian Physical Tables.[4] The first part of the emittance data was taken in the course of the angular distribution measurements where the ribbon temperature was maintained for approximately one hour at each 100 degree increment; the same ribbon being used in its initially polished state on through the upper temperature limit and having no previous heating history prior to this run. Because of the rather large elapsed time, the surface of the metal had an opportunity to undergo some thermal etching and grain reorientation, and thus the data contains a hidden temporal variation as well as a temperature variation of emittance.

Figures 11 and 12 are graphs of the angular distribution of intensity relative to the normal, plotted against the angle θ and cos θ, respectively, at 870°K and 1490°K. After completion of the high temperature runs the angular distribution was measured again at 870°K and a decrease of approximately 1% in the ratio at this temperature was noted. This could be attributed to surface changes during the elevated temperature runs. The departure from Lambert's cosine law can be seen in Figs. 11 and 12. In Fig. 12 the ratio of total hemispherical emittance to total normal emittance can be visualized easily as the area under the experimentally observed curve. The area defined by the straight line segments is equal to unity. Although it is only necessary to measure the distribution in the interval $0 \leq \theta \leq 90^\circ$ to find the ratio, it was found advantageous to use the interval $-90^\circ \leq \theta \leq 90^\circ$ so that the effect of angular misalignment would be averaged as well as affording a check on possible spurious reflections. The ratio as obtained by these angular distribution curves is plotted against temperature in Fig. 13 along with the ratio obtained by dividing the electrical power dissipation by the thermopile voltage and an appropriate calibration factor. This ratio is shown as a function of total normal emittance in Fig. 14. The dashed curve is the theoretical ratio obtained from Equations (1) and (2).

The experimental values of the total hemispherical and total normal emittance are shown in Fig. 15 along with the theoretical curves based on Equations (1) and (2). The total normal emittance was obtained by the thermopile deflections and Equation (14) and also by dividing the total hemispherical emittance by the ratio obtained by the angular distributions (circles in Fig. 13). The data in Fig. 15 are plotted on a compressed scale in Fig. 16 to show the possibility of representing the results to within ±5% by direct proportionalities between the emittances and the absolute temperature. These relationships are

$$\epsilon_H = 1.22 \times 10^{-4}\ T(^\circ K)$$

$$\epsilon_N = 1.03 \times 10^{-4}\ T(^\circ K)$$

where the coefficients have units of deg^{-1}.

Spectral emittance data as determined with the optical pyrometer and thermocouple according to Equation (16) are shown in Fig. 17.

During the angular distribution measurements at 1390°K and 1490°K, the brightness temperature of the ribbon underwent some startling changes. As the true temperature of 1390°K was initially reached, the brightness temperature was uniform over the ribbon, but after 15 - 20 minutes the surface took on a "salt and pepper" appearance, having three distinct apparent temperatures at 1292°K, 1305°K, and 1323°K. The range of apparent spectral emittances is indicated by the dashed lines in Fig. 17. The relative areas of these temperature regions initially were about equal and considerably less than a millimeter square. As time progressed, the relative areas changed to where the 1305°K temperature was predominant at the end of the run. These changes in brightness temperature were accompanied by almost negligible changes in true temperature and total hemispherical emittance while the current through the ribbon was held constant. When the thermocouple temperature was raised to 1490°K, two brightness temperatures were observed; one at 1390°K, the other at 1404°K. The area of the 1404°K region diminished with time until at the end of the run, the ribbon was again uniform at 1390°K. At 1490°K thermocouple temperature, a 4C° drop in the thermocouple temperature was observed during the course of the run while the current was held constant corresponding to a 1.1% rise in total hemispherical emittance.

In order to investigate the effect of time, measurements of emittance versus temperature during four consecutive temperature cycles on a single sample of platinum were made in the stationary thermopile system. The total time for all four runs was approximately eight hours. Fig. 18 is a plot of the experimentally determined values of the total emittance along with their theoretical values taken from Equations (1) and (2) and the measured values of electrical resistivity. The lowest curves (average of cycles 2 and 3) are the most representative of the emittance of the polished sample, since cycle 1 had to be omitted because of instrumental difficulties. The changes were between 5% and 10% for the total sequence.

The change in spectral emittance at 0.65 micron is illustrated in Fig. 19. During the rising part of the first heating cycle the spectral emittance is seen to decrease with temperature. However, there is also a change in the surface taking place during the run because the spectral emittance at 800°K is considerably lower at the end of the first cycle than it was at the beginning. It then rises appreciably during the succeeding temperature cycles. During these runs the electrical resistivity did not change as can be seen in Fig. 20.

A second platinum strip was held at 1285°K while the total hemispherical emittance and the spectral emittance were observed as a function of time. The results of this test are shown in Fig. 21. The initial values of these emittances are higher since the ribbon was not as specular to begin with as the one used in the cyclic tests.

Photomicrographs of a platinum strip before heating and after it had been held at about 1500°K for 4.5 hours are shown in Fig. 22.

DISCUSSION

Instrumentation has been designed, fabricated, and tested for the measurements, over a wide temperature range, of the total hemispherical emittance, total normal emittance, angular distribution of total radiation, and the spectral emittance at 0.65 micron on a single surface of an electrically heated metallic strip. The estimated overall accuracy of the system is ±5%. A slight drift of the thermopile output voltage has given rise to the largest systematic uncertainty of the apparatus. This is due primarily to ambient temperature changes of the thermopile housing (e.g., the cold junction) and the bell jar which forms the background of the sample in the field of view of the thermopile. Since the thermopile is used as an absolute device in the determination of the normal emittance, some uncertainty exists in this measurement. However, the error is still within the ±5% quoted for the system. Modifications have been planned for extending the upper temperature limit of the experimental appartus to 2700°K which requires a regulated power capability of 10 kilowatts. Water cooling will be provided for the thermopile housing and the sample background as well as for the other components which might be adversely affected by the high temperature.

It is extremely important in the determination of the total normal emittance that the radiation thermopile have a flat spectral response. In the present system there were no optical elements between the detector and the ribbon, only field of view stops. The thermopile was coated with an aqueous solution of lamp black. The flat spectral response of the system was demonstrated in Fig. 9 by the linearity of the thermopile voltage versus electrical power dissipation from a diffusely radiating strip (angular distribution of radiation obeying the cosine law) as it was brought through a wide temperature range.

In addition to developing the instrumentation some pertinent data was obtained on the radiating properties of platinum between 800°K and 1500°K. The results of this research to date have shown that in the temperature range investigated, the total hemispherical emittance (the important parameter of radiant heat transfer) of platinum can be well represented by the direct proportionality

$$\epsilon_H = 1.22 \times 10^{-4} T(^\circ K)$$

where the coefficient has units of $\deg^{-1}$. This is about 18% higher than the total normal emittance which is more commonly measured, and it deviates both positively and negatively by about 10% from the theoretical equation of Davisson and Weeks (Equation 2). Although the underlying reason for this direct proportionality is not understood, it is not surprising that the agreement with Equation (2) may be off by 10%. A comparison of the NRDL data with the experimental results of Davisson and Weeks along with their theoretical curve appears in Fig. 23. The difference between the experimental curves may be partly due to the difference in surface quality of the wire and the ribbon. Some of the discrepancy between the experimental and theoretical curves in Fig. 16 is undoubtedly due to the use of the steady field bulk resistivity in Equation (2) instead of the electrical resistivity close to the surface at infrared frequencies.

According to Fig. 10 the value of ρ/T is about 3.5×10^{-8} which is clearly a violation of the approximation given in Equation (10). This means that the period of an appreciable portion of the electromagnetic radiation is shorter than the relaxation time of the electrons. Under these circumstances the current is not in phase with the electric field, and this results in a higher reflectivity according to the treatment of Mott and Jones.[21] Then, for a given steady field electrical resistivity, the emissivity would be lower than that given by Equation (2). The magnitude of this correction has not been worked out, but it is in the right direction to produce better agreement with the experimental curve at low temperatures. However, the agreement at high temperatures would be even poorer. The resistivity at the surface would be expected to be higher than the bulk resistivity, but such a correction would be likely to increase the emissivity at low temperatures by a larger factor than at high temperatures. The high temperature discrepancy may be due to the large value of the second term in Equation (2). It is possible that this term is too high in view of the violation of the underlying assumption expressed in Equation (10). At any rate it is apparent that Equation (1) and Equation (2) should be modified to take the relaxation time of the electron into account. While some increase in the total hemispherical emittance at high temperatures was undoubtedly due to surface changes during the runs, the final measurements, which repeated the low temperature data, indicated emittance increases of less than 5%. Another possible source of error is the neglecting of the short wavelength effects caused by the bound electrons and the internal photoelectric effect. At low temperatures these effects are not important since there is not a significant amount of radiation taking place at these wavelengths.

It was found that if a platinum surface is held at 0.6 times its melting temperature for several hours, an increase of up to 5% can be expected in its total hemispherical emittance due to thermal etching and recrystallization at its surface. Measurements of the equilibrium changes in emittance as a function of temperature should be made up to larger fractions of the melting point than the one determination quoted here. This will be done in the study of the refractory metals.

The change in surface geometry due to recrystallization is noted in Fig. 22. The width of the boundary of the crystallites is very small, which may lead to a selective wavelength effect in emission. At the wavelength of the optical pyrometer these zones might act more or less like black radiators, and thus there would be an increase in the spectral emittance at 0.65 micron. However, these zones would be too narrow to contribute significantly in the wavelength regions where most of the radiation occurs. Hence, a much larger effect on the spectral emittance than on the total emittance would be expected.

It is difficult to explain the decrease in spectral emittance with temperature during the first cycle in Fig. 21 and then its increase with temperature on subsequent runs. However, both types of behavior have been reported by previous workers.[17]

REFERENCES

1. W. N. Harrison, J. C. Richmond, E. K. Plyler, R. Stair, and H. K. Skramstad, "Standardization of Thermal Emittance Measurements", WADC Technical Report 59-510, August 1959.

2. E. Aschkinass, Ann. Phys. Lpz. *17*, 960, (1905).

3. P. D. Foote, Bull. Nat. Bur. Stand. *11*, 607 (1914/1915).

4. W. E. Forsythe, Smithsonian Physical Tables, 9th Edition, Smithsonian Institute, 1954.

5. C. Davisson and J. R. Weeks, J. Opt. Soc. Amer. *8*, 581 (1924).

6. N. F. Mott and H. Jones, "*The Theory of the Properties of Metals and Alloys*", 1st Edition, p. 63, Oxford University Press, 1936.

7. Van Vleck, "*Electric and Magnetic Susceptibilities*", p. 225, Oxford University Press, 1932.

8. H. G. Van Bueren, "Imperfections in Crystals", p. 454, North-Holland Publishing Co., Amsterdam, 1960.

9. F. Seitz, *The Physics of Metals*, p. 81, McGraw-Hill Book Co., Inc., New York, 1943.

10. R. Hultgren, *Physical Metallurgy*, p. 162, Prentice-Hall, Inc., New York, 1953.

11. D. McLean, *Grain Boundries in Metals*, p. 252, Oxford at the Clarendon Press, 1957.

12. G. Sachs, K. R. Van Horn, *Practical Metallurgy*, p. 126, The American Society for Metals, 1952.

13. R. L. Fullman, *Metal Interfaces*, p. 179, American Society for Metals, 1952.

14. L. Delisle, G. A. Davis, *The Physics of Powder Metallurgy*, p. 214, McGraw-Hill Book Co., Inc., New York, 1951.

15. J. C. DeVos, The Emissivity of Tungsten Ribbon, Thesis, Amsterdam 1953.

16. N. F. Mott, and C. Zener, Cambridge Philosophical Society Proceedings, p. 268, 30, 1934.

17. G. A. W. Rutgers, Encyclopedia of Physics, Vol. XXVI, p. 150, Springer-Verling, Berlin, 1958.

18. A. G. Worthing, Temperature, Its Measurement and Control in Science and Industry, Fig. 12, p. 1180, Reinhold Publishing Corp., New York, 1941.

19. Metals Handbook, p. 1123, American Society for Metals, 1948.

20. American Institute of Physics Handbook, p. 4-13, McGraw-Hill Book Co., 1957.

21. N. F. Mott and H. Jones, Properties of Metals and Alloys, 1st Edition, p. 112, Oxford University Press, 1936.

Table 1

Emittance and Resistivity Data During Angular Distribution Measurements

Temperature °K	ϵ_H	ϵ_H/ϵ_{N1}	ϵ_{N1}	ϵ_{N2}	ϵ_H/ϵ_{N2}	ϵ_λ	ρ
774	0.095	1.220	0.0780	0.076	1.25	--	28.5
873	0.1050	1.224	0.0857	0.086	1.22	--	30.9
873	0.1085	1.209	0.0898	0.090	1.21	--	31.0
991	0.1205	1.190	0.1013	0.101	1.195	--	35.1
1054	0.1255	1.199	0.1046	0.1065	1.18	0.265	37.0
1091	0.133	1.181	0.1125	0.1125	1.18	0.287	38.3
1095	0.1315	1.193	0.1103	0.1105	1.19	0.298	38.4
1193	0.1460	1.183	0.1233	0.123	1.185	0.312	41.9
1293	0.1587	1.178	0.1350	0.136	1.17	0.329	44.4
1389	0.1680	1.170	0.1435	0.142	1.18	0.336-0.394	46.8
1493	0.1840	1.171	0.1570	0.157	1.17	0.354-0.378	50.2

ϵ_H: Total hemispherical emittance determined from electrical power dissipation

ϵ_H/ϵ_{N1}: Ratio total normal to total hemispherical emittance obtained from angular distribution of radiation

ϵ_{N1}: ϵ_H divided by ϵ_H/ϵ_{N1}

ϵ_{N2}: Total normal emittance obtained with thermopile

ϵ_λ: Spectral emittance at 0.65 micron

ρ: Electrical resistivity in micro-ohms cm

Table 2

Electrical Resistivity Data During Several Temperature Cycles

Cycle 2 Up*		Cycle 3 Up		Cycle 4 Up		Cycle 4 Down	
T°K	ρ	T°K	ρ	T°K	ρ	T°K	ρ
778	29.39	771	29.62	765	29.22	842	32.38
847	32.59	849	32.59	897	34.16	958	35.74
911	34.16	910	34.16	962	35.54	1058	39.29
961	35.32	964	35.56	1014	38.11	1198	43.83
1015	38.14	1016	38.14	1061	39.10	1279	46.21
1062	39.08	1064	39.08	1112	40.48	1356	48.18
1111	40.25	1161	41.89	1158	42.06	1429	50.16
1159	41.66	1248	44.24	1203	43.44	1467	50.35
1206	43.85	1330	46.40	1247	44.62		
1250	44.39	1406	48.62	1287	46.01		
1291	45.41	1476	49.94	1325	46.79		
1330	46.43			1363	48.18		
1369	46.97			1399	49.17		
1406	48.77			1435	50.16		
1445	49.94			1467	50.35		
1480	50.34						

ρ: Electrical resistivity in micro-ohm cm

*Cycle 1 was unusable for Resistivity Data.

Table 3

Total Normal Emittance Data
During Several Temperature Cycles

Cycle 3 Up*		Cycle 4 Up		Cycle 4 Down	
T°K	ϵ_N	T°K	ϵ_N	T°K	ϵ_N
1016	.1056	1014	.1058	1058	.1161
1064	.1136	1061	.1147	1198	.1381
1161	.1249	1112	.1237	1279	.1494
1248	.1368	1158	.1283	1356	.1588
1330	.1456	1203	.1336	1429	.1665
1406	.1537	1247	.1385		
1476	.1628	1287	.1437		
		1325	.1487		
		1363	.1540		
		1399	.1584		
		1435	.1633		
		1467	.1686		

ϵ_N: Total normal emittance obtained with a thermopile

*Normal emittance data not taken during cycles 1 and 2.

Table 4

Total Hemispherical Emittance Data During Several Temperature Cycles

Cycle 2 Up*		Cycle 3 Up		Cycle 4 Up		Cycle 4 Down	
$T^{o}K$	ϵ_H	$T^{o}K$	ϵ_H	$T^{o}K$	ϵ_H	$T^{o}K$	ϵ_H
1015	.1295	1016	.1294	1014	.1300	1058	.1400
1062	.1365	1064	.1358	1061	.1375	1198	.1600
1111	.1428	1161	.1474	1112	.1465	1279	.1725
1159	.1481	1248	.1589	1158	.1498	1356	.1830
1206	.1557	1330	.1688	1203	.1588	1429	.1933
1250	.1586	1406	.1793	1247	.1610		
1291	.1634	1476	.1868	1287	.1676		
1330	.1688			1325	.1730		
1369	.1740			1363	.1790		
1406	.1799			1399	.1850		
1445	.1835			1435	.1904		
1480	.1865			1467	.1933		

ϵ_H: Total hemispherical emittance obtained from electrical power dissipation

*Cycle 1 was unusable for hemispherical emittance values.

Table 5

Spectral Emittance Data at 0.65 Micron During Several Temperature Cycles

Cycle 1 Up		Cycle 3 Up*		Cycle 4 Up		Cycle 4 Down	
T°K	ϵ_λ	T°K	ϵ_λ	T°K	ϵ_λ	T°K	ϵ_λ
1045	.3546	1064	.3054	1061	.3307	1058	.3512
1095	.3804	1161	.3177	1112	.3086	1198	.3804
1145	.3546	1248	.3443	1158	.3410	1279	.4079
1170	.3804	1330	.3274	1203	.3443	1356	.4162
1234	.3654			1247	.3547	1429	.4421
1278	.3477	1476	.3692	1287	.3477		
1321	.3374			1325	.3654		
1362	.3582			1363	.3729		
1406	.3307			1399	.3921		
1443	.3443			1435	.3999		
1479	.3374			1467	.4121		

ϵ_λ: Spectral emittance at 0.65 micron obtained with an optical pyrometer.

*Spectral emittance data not taken during cycle 2 up.

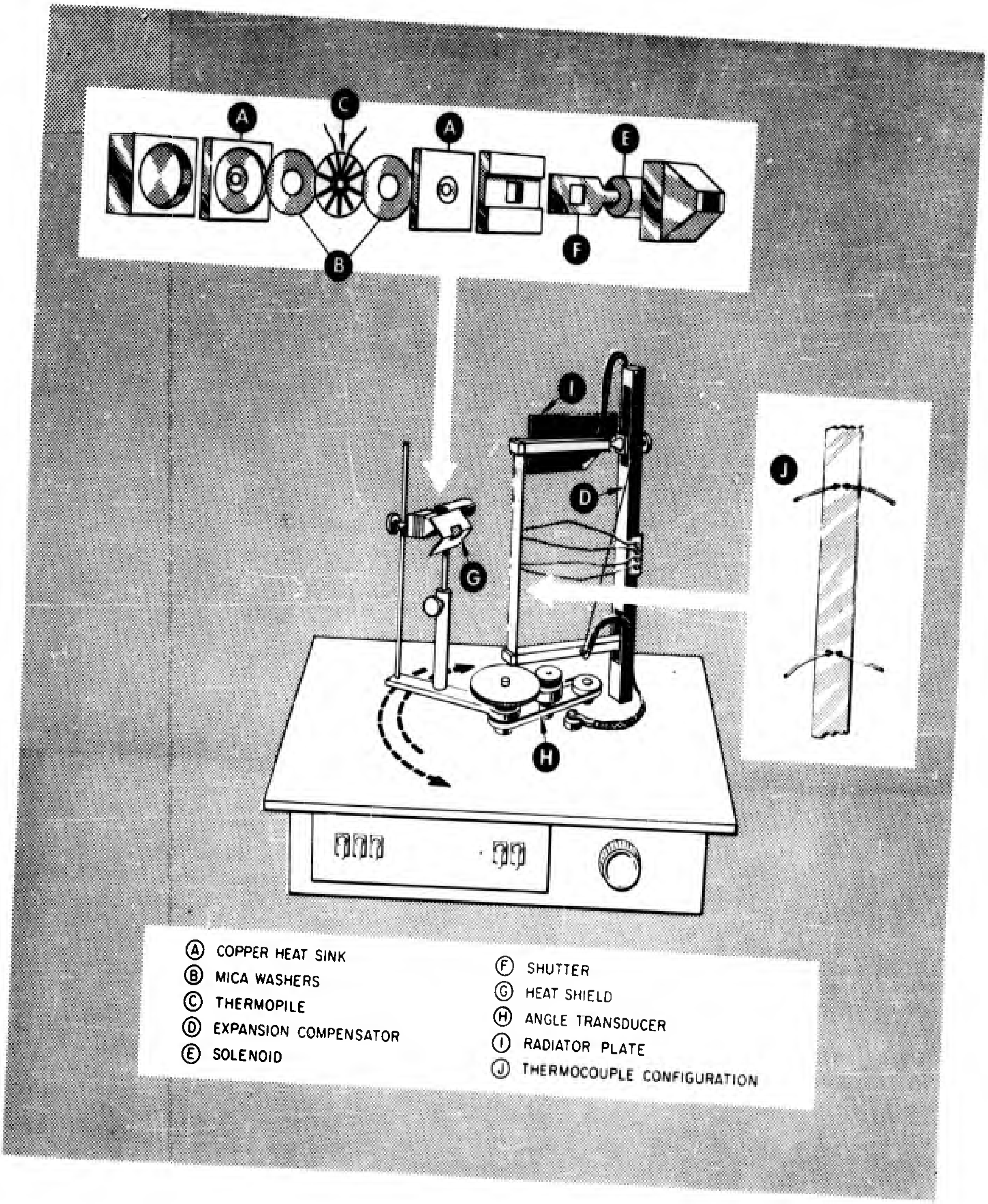

Fig. 1 Schematic diagram of experimental arrangement for measuring angular distribution.

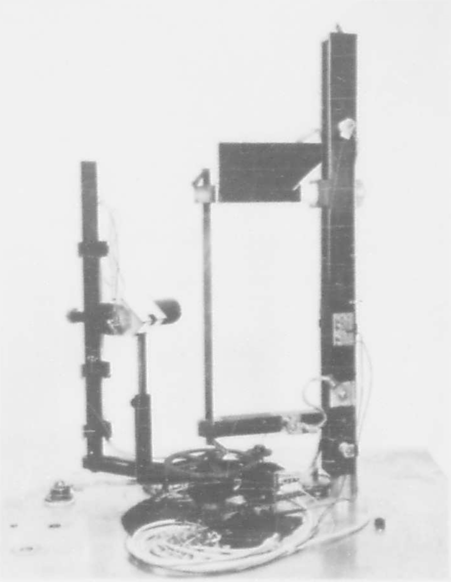

Fig. 2 Detail photograph of apparatus for measurement of angular distribution.

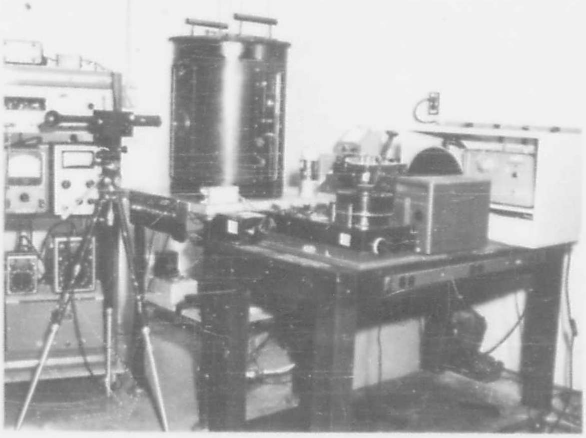

Fig. 3 Over-all photograph of apparatus for measurement of angular distribution.

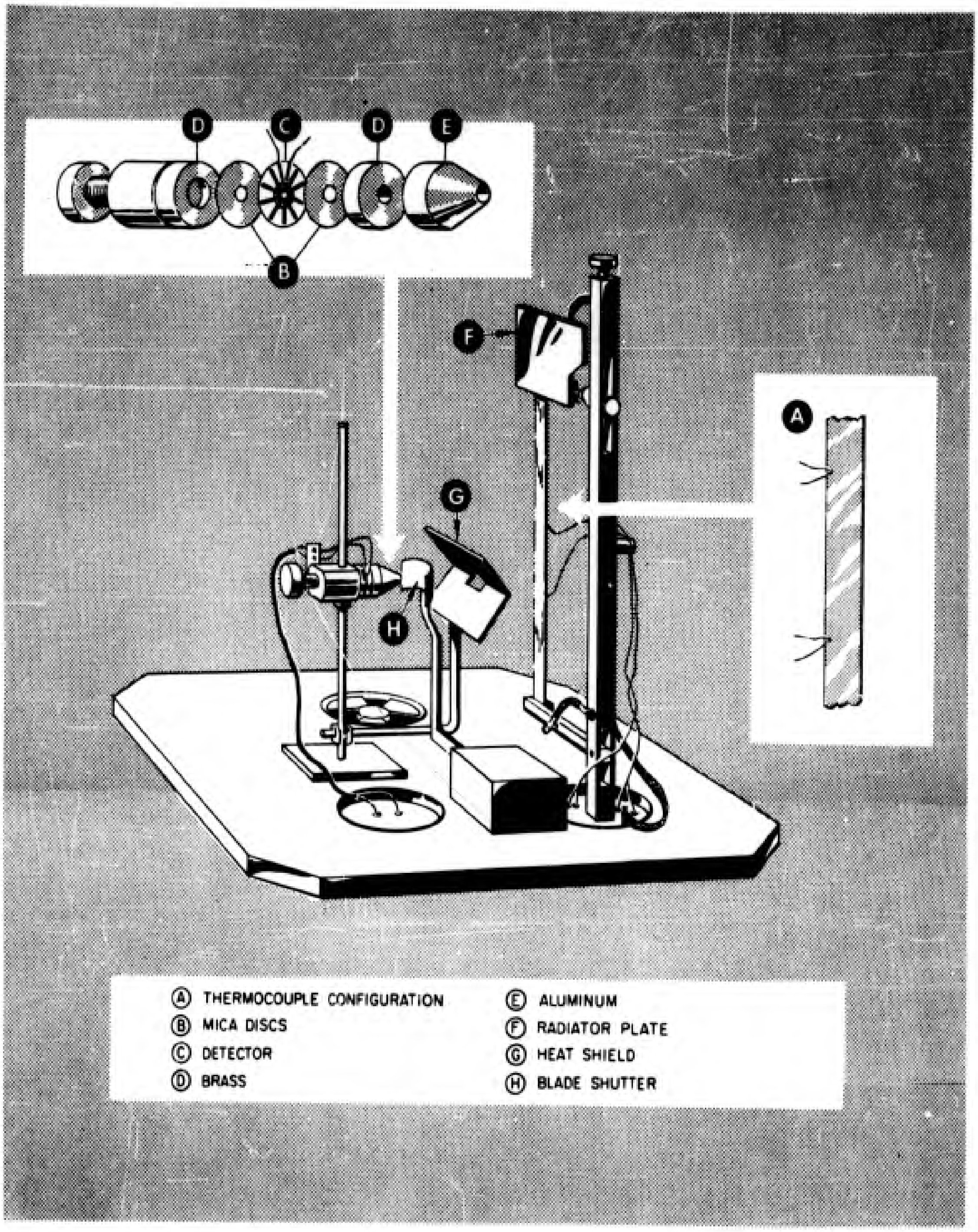

Fig. 4 Schematic diagram of experimental arrangement for measurement of time dependence of emittance.

Fig. 5 Detail photograph of apparatus for measurement of time dependence of emittance.

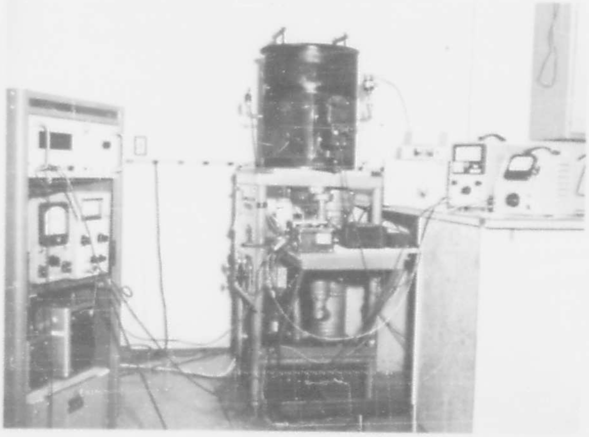

Fig. 6 Over-all photograph of apparatus for measurement of time dependence of emittance.

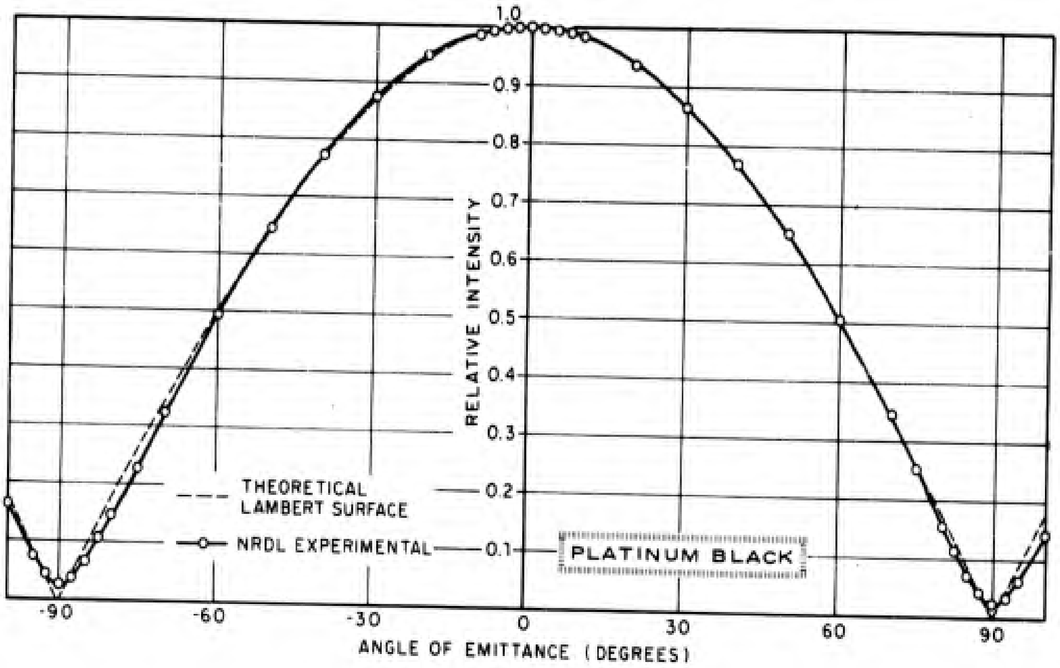

Fig. 7 Intensity relative to normal intensity of a platinum-black surface versus angle of emittance.

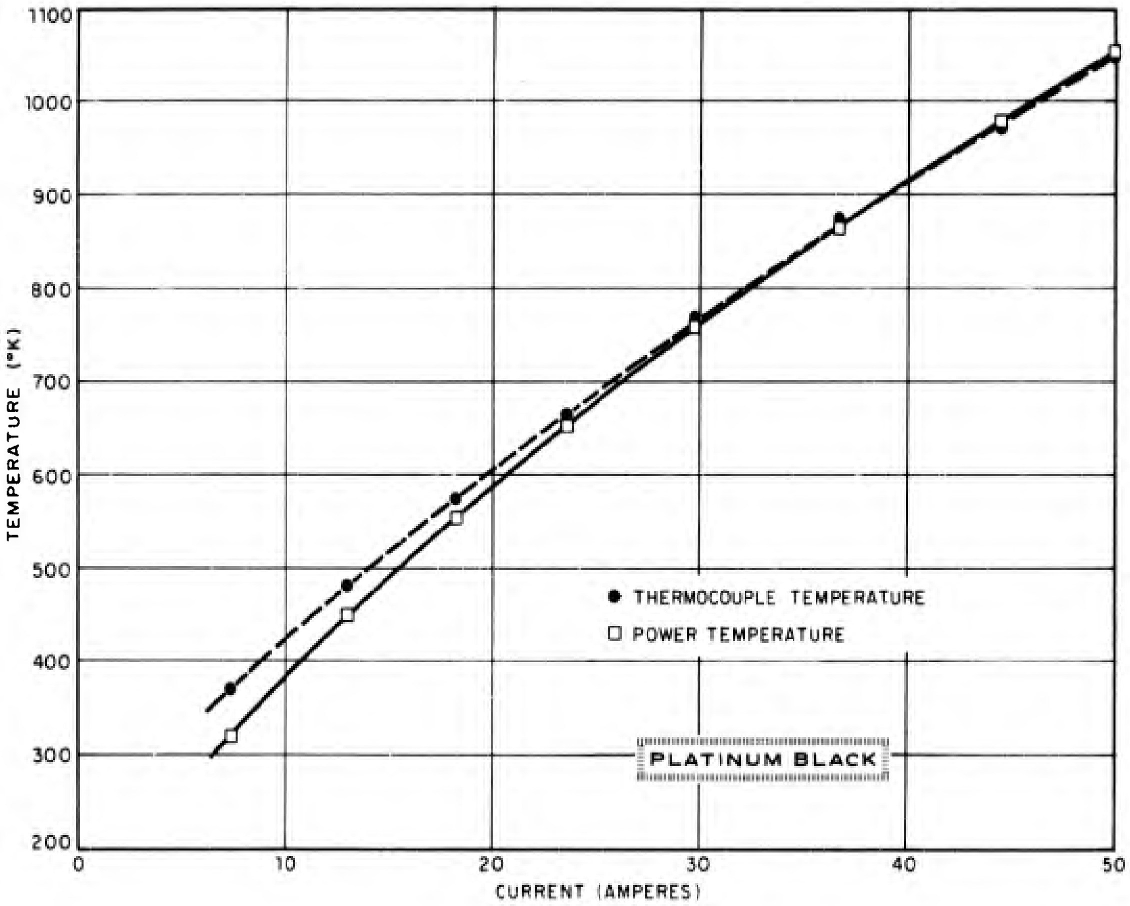

Fig. 8 Comparison of the thermocouple and power temperatures versus current, in a platinum blackened ribbon.

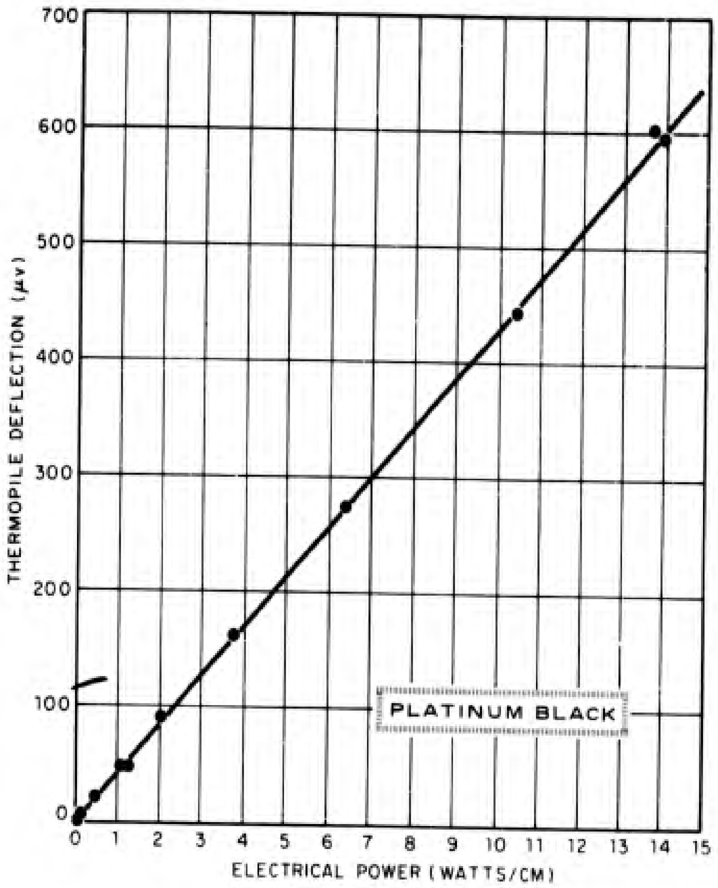

Fig. 9 Thermopile deflection (μv) versus electrical power (watts/cm) in a platinum blackened ribbon.

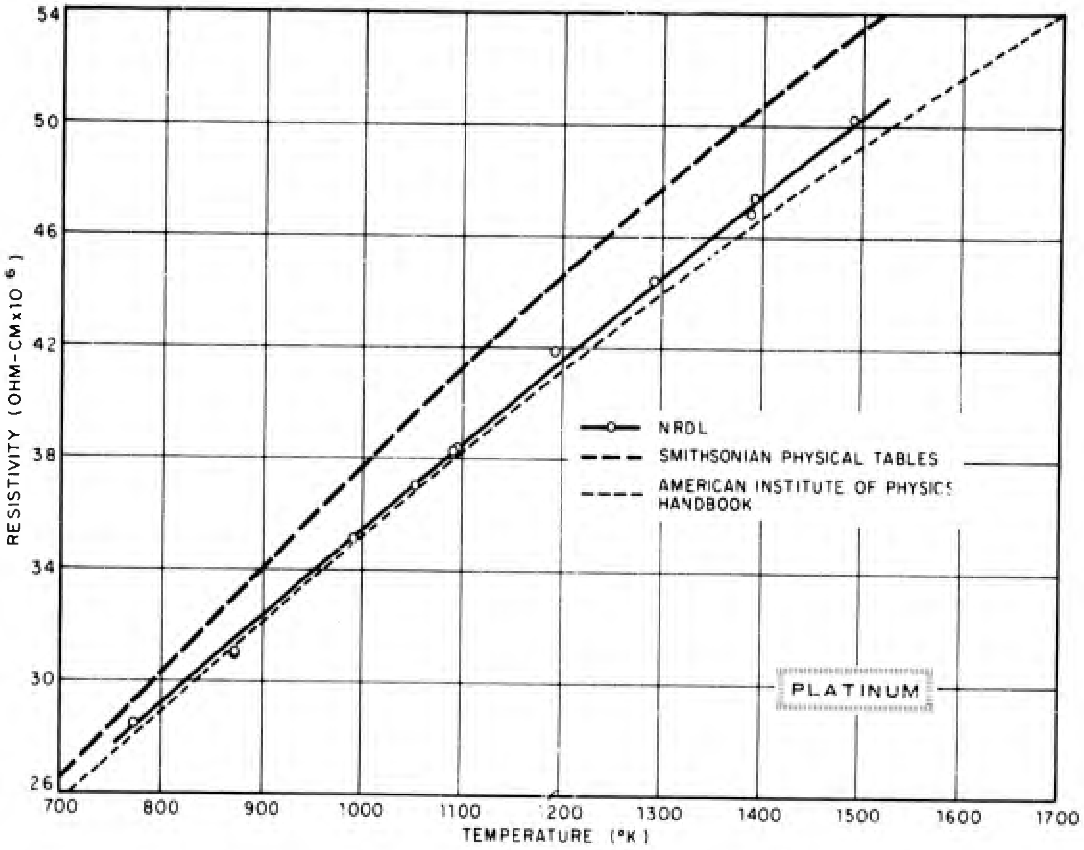

Fig. 10 Resistivity versus absolute temperature.

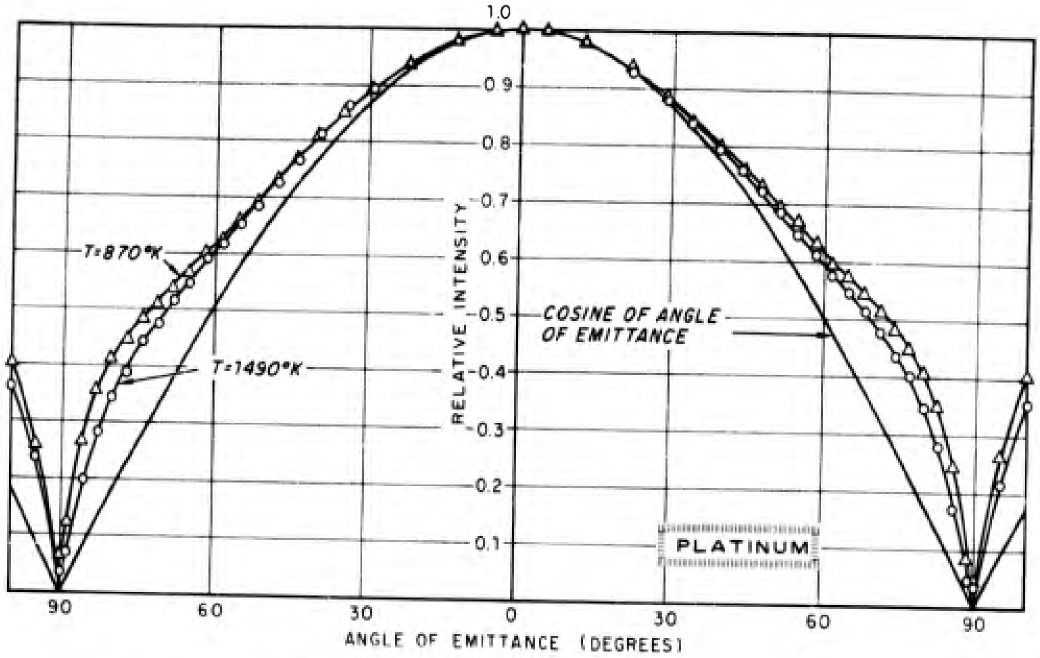

Fig. 11 Intensity relative to normal intensity versus angle of emittance.

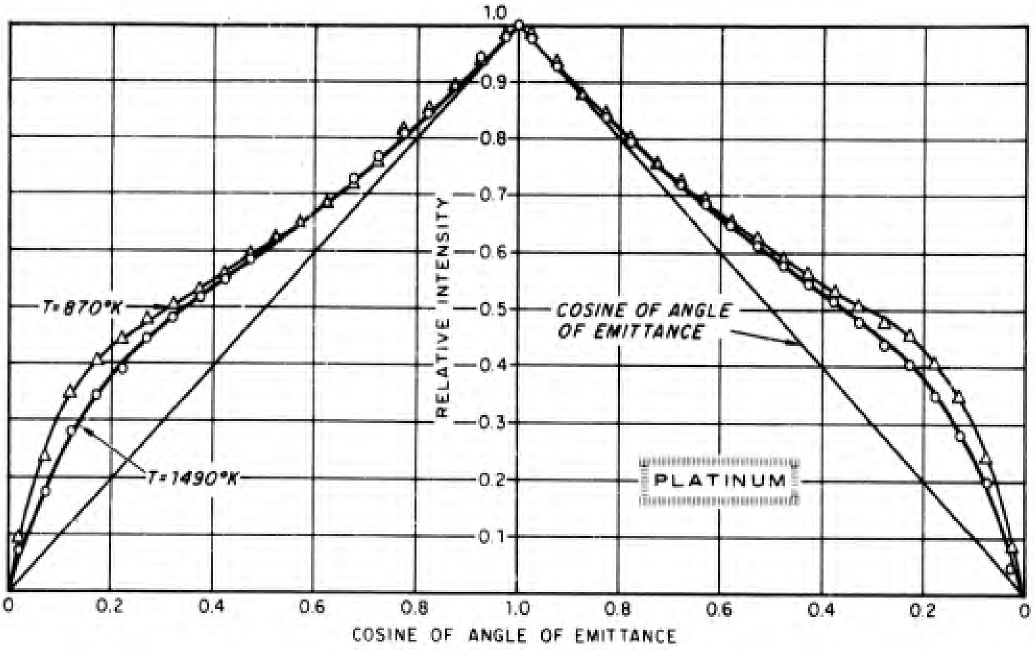

Fig. 12 Intensity relative to normal intensity versus cosine of angle of emittance.

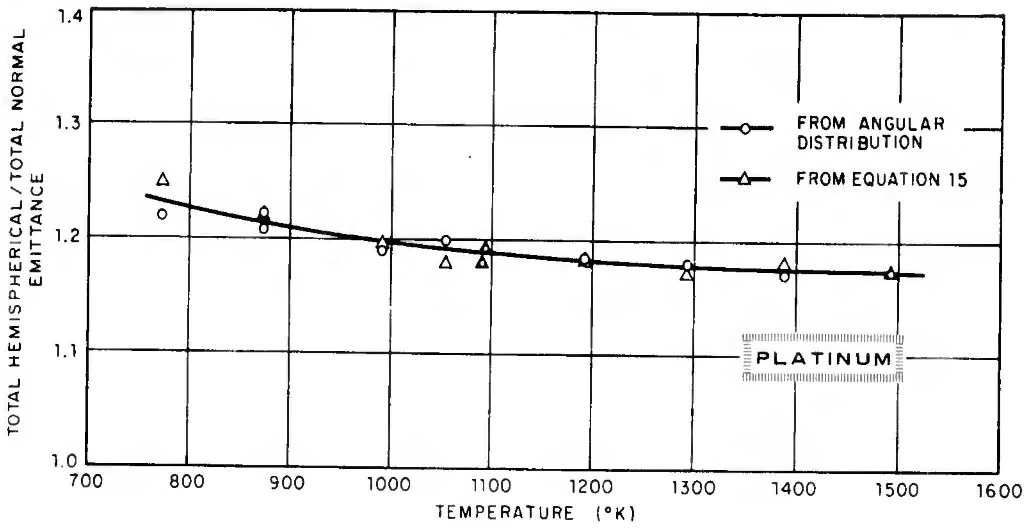

Fig. 13 Ratio of total hemispherical to total normal emittance versus absolute temperature.

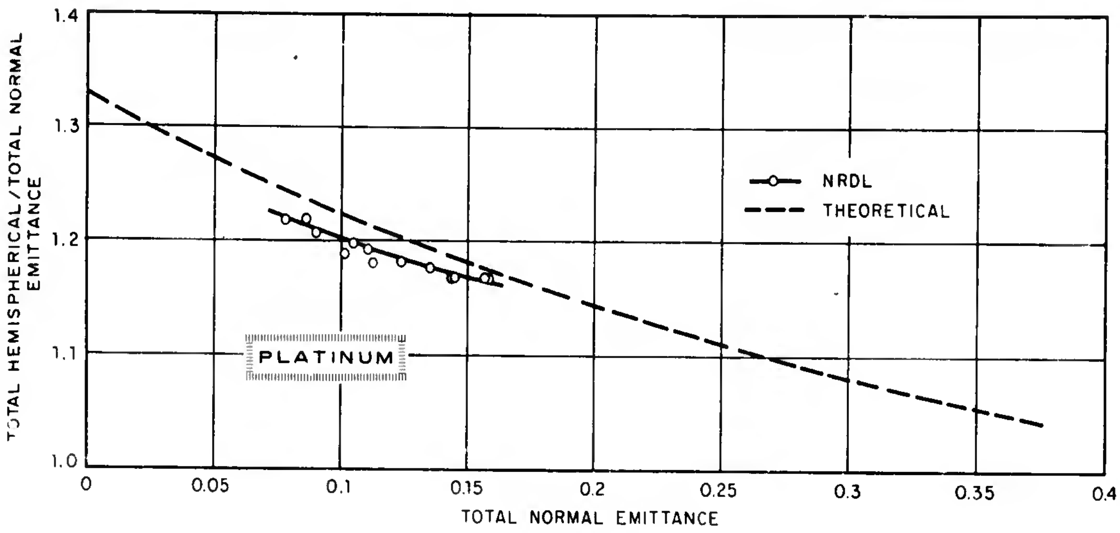

Fig. 14 Ratio of total hemispherical to total normal emittance versus total normal emittance.

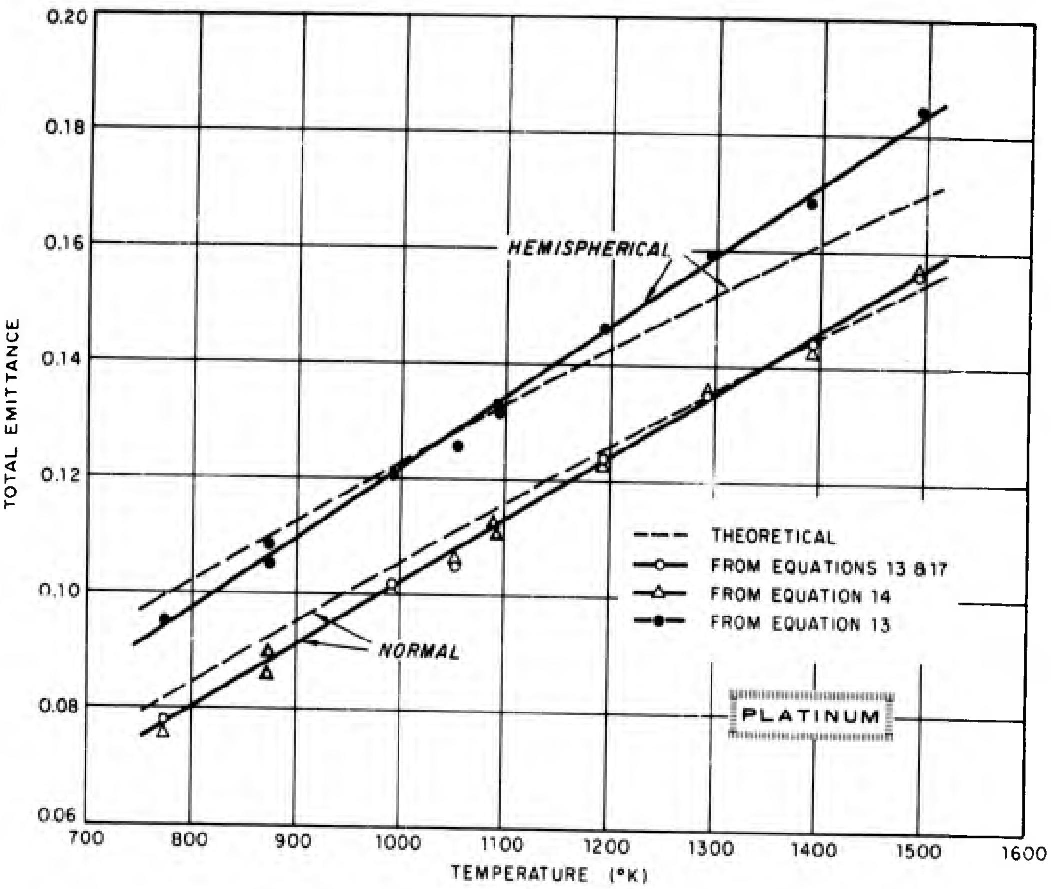

Fig. 15 Total hemispherical and total normal emittance versus absolute temperature.

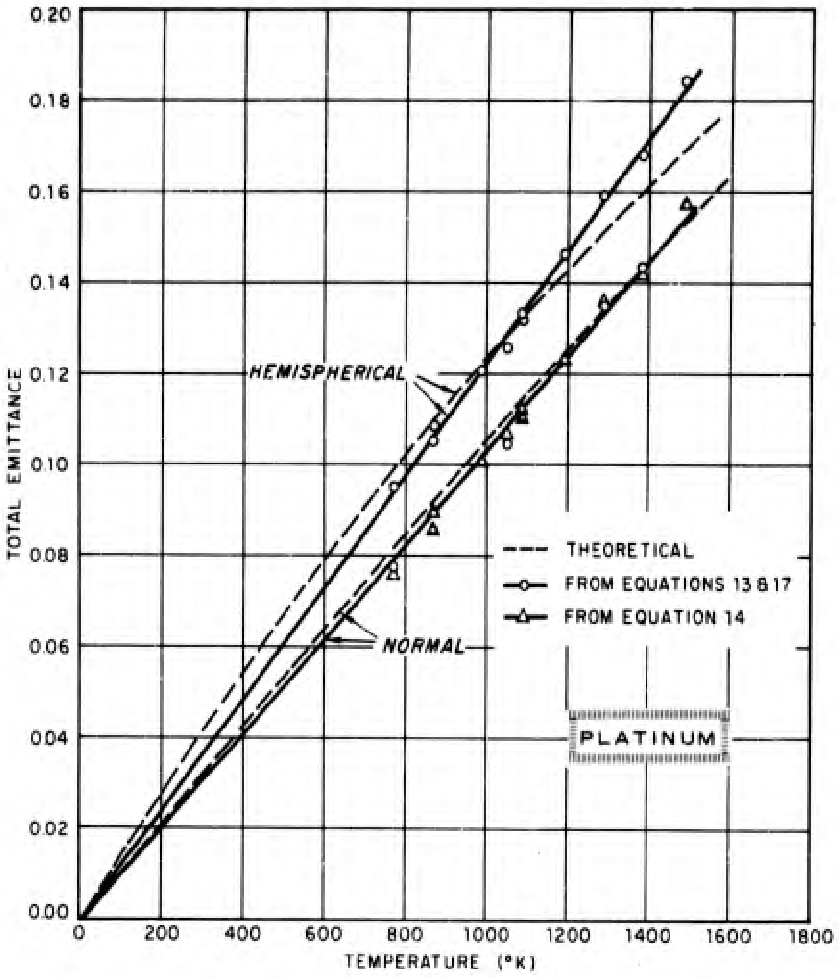

Fig. 16 Total hemispherical and total normal emittance versus absolute temperature linearly extrapolated to zero.

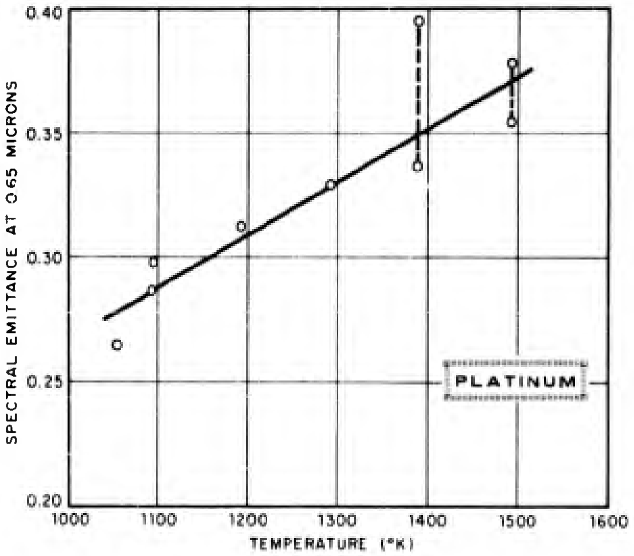

Fig. 17 Spectral emittance at 0.65 micron versus absolute temperature.

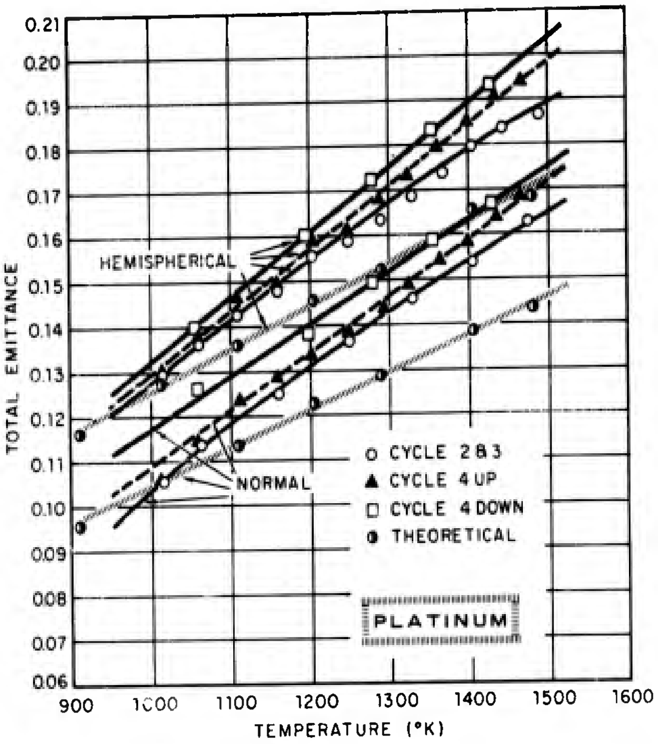

Fig. 18 Total emittance versus absolute temperature illustrating the effects of surface changes with time.

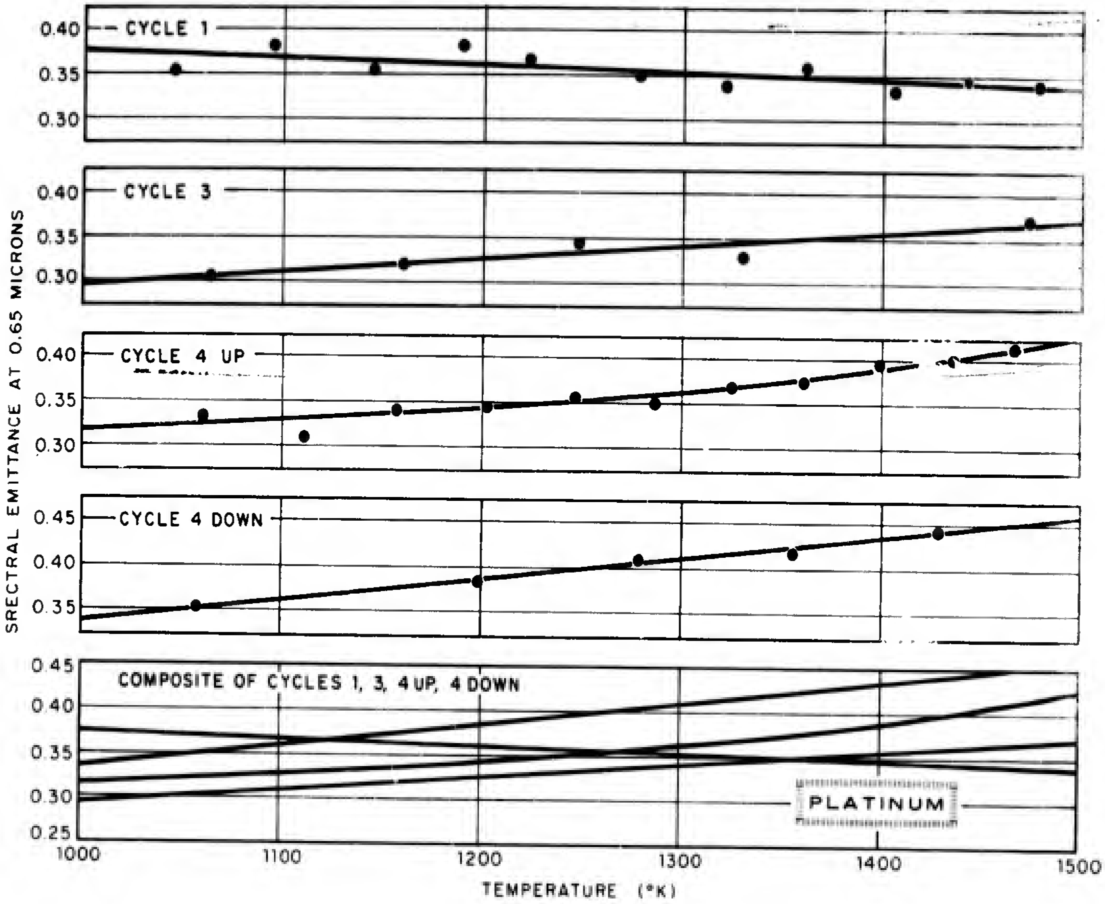

Fig. 19 Spectral emittance at 0.65 micron versus absolute temperature illustrating the effects of surface changes with time.

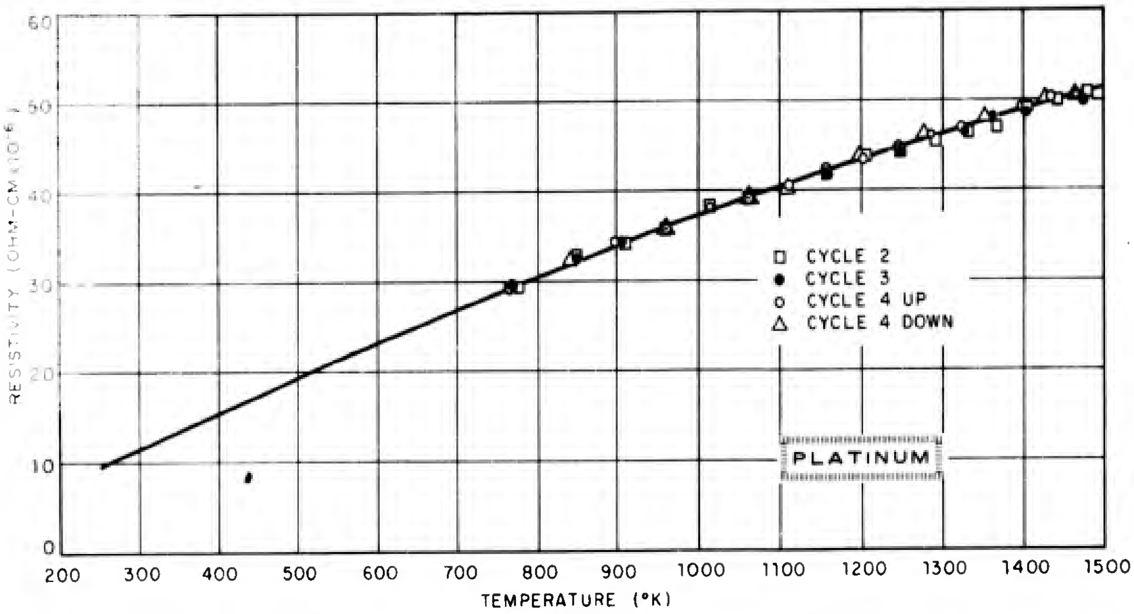

Fig. 20 Resistivity versus absolute temperature during several temperature cycles.

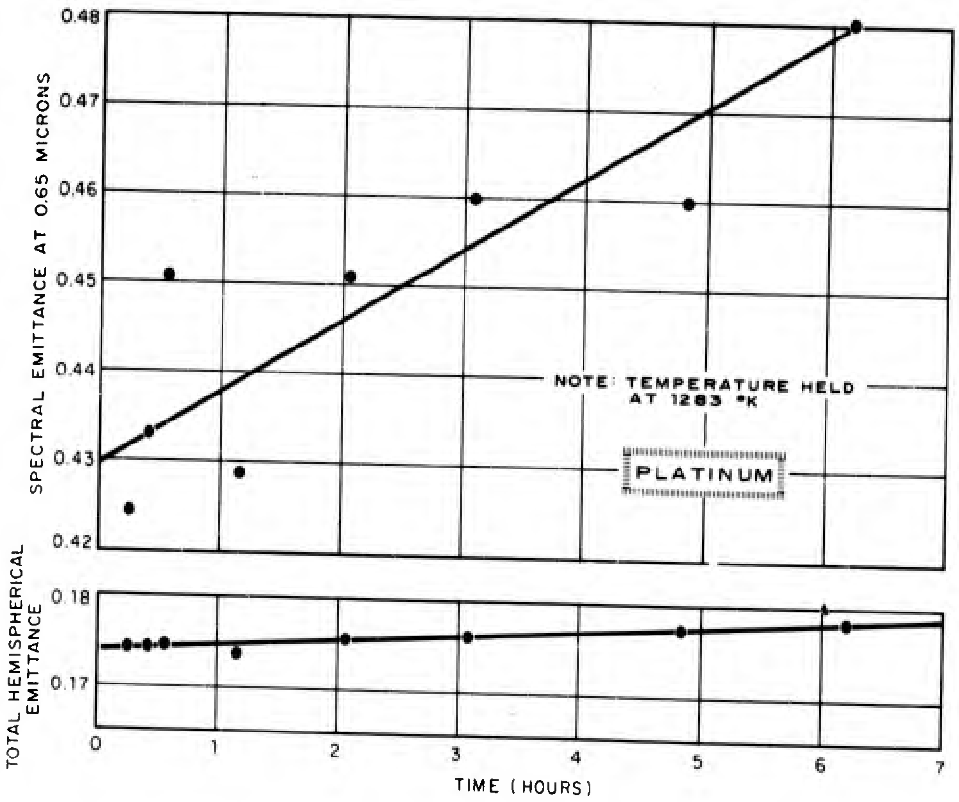

Fig. 21 Spectral emittance at 0.65 micron and total hemispherical emittance versus time at 1283°K.

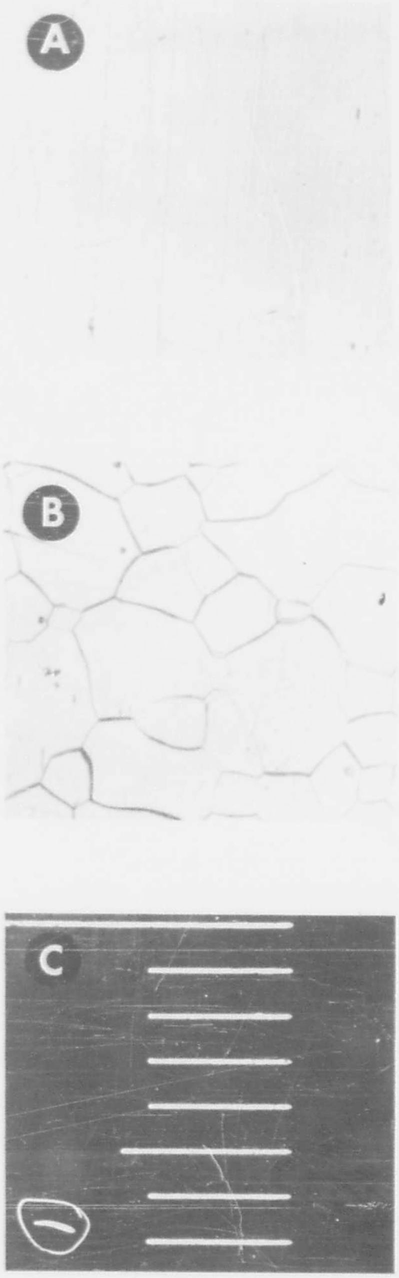

Fig. 22 Photomicrographs of the platinum surface: (a) as received, (b) after 4.5 hours at ≈ 1500°K, (c) scale with 100 micron separation between marks.

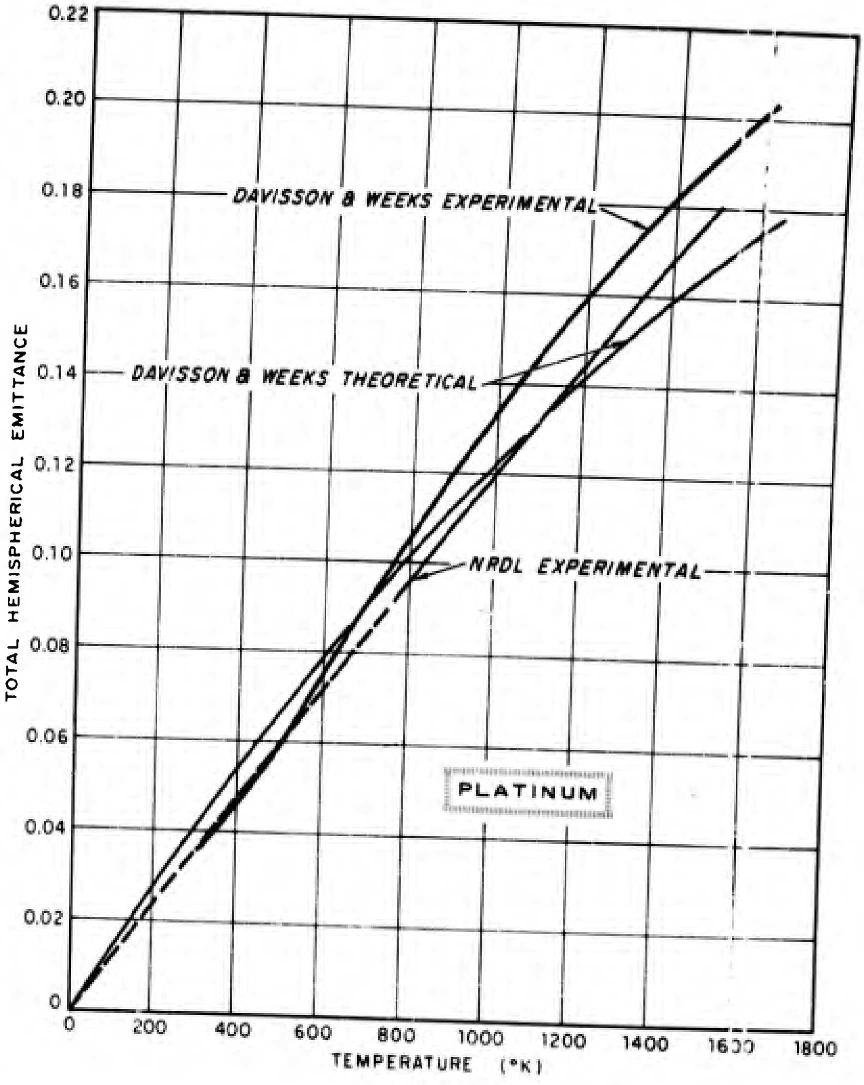

Fig. 23 Comparison of the total hemispherical emittance versus temperature measurements of Davisson and Weeks and NRDL.